Short Papers

Indirect Adaptive Control of an Electrohydraulic Servo System Based on Nonlinear Backstepping

Claude Kaddissi, Jean-Pierre Kenné, and Maarouf Saad

***Abstract*—This paper studies the real-time position control of an electrohydraulic system using indirect adaptive backstepping. Electrohydraulic systems are known to be highly nonlinear and nondifferentiable. Backstepping is used for being a powerful, nonlinear control strategy and for its ability to ensure an asymptotic stability of the controlled system without canceling useful nonlinearities. On the other hand, hydraulic parameters are prone to variations; it is, therefore, useful to employ an adaptive control strategy in order to update the controller with the parameters variation. In such a case, indirect adaptive control is highly recommended, among other adaptive controller types, as it has the benefit of identifying the real system parameters value. Since not much literature is available for the indirect method as applied to the hydraulic systems, because of its implementation complexity, this paper shows how efficiently this method can handle the parameter estimates.**

***Index Terms*—Adaptive control, backstepping, electrohydraulic systems, nonlinear control.**

I. Introduction

Currently electrohydraulic systems are very popular in many industrial processes, including heavy machinery, robotics, aircraft, and automotive. This is principally due to the high power-to-volume ratio that these systems can offer. However, the nonlinearities and the mathematical model singularity of electrohydraulic systems result in traditional constant gain controllers being inadequate.

There are two issues at stake when dealing with electrohydraulic systems: the accuracy of the mathematical model and the effectiveness of the control strategy. Regarding the first issue, basic modeling of hydraulic components is addressed in [1] where the most crucial dynamics and parameters are taken into consideration. Since then, several improvements were made: for example, in [2], a new design for asymmetric linear hydraulic actuators is developed, while a dynamic redesign of a nonlinear servovalve is considered in [3]–[5]. The mathematical model that we adopted in this paper is inspired from the previous work, with some improvements brought in.

Regarding the control issue, several classical and advanced strategies can be found in the literature. Among linear control strategies, pole placements and classic proportional–integral–derivative (PID) controller are used in [6] and [7], respectively. Likewise, more efficient nonlinear control strategies are widely in use, like sliding mode control in [8] and [9], input–output linearization that was adopted in [10], and nonlinear backstepping as applied in [11] for position tracking and in [12] for force tracking. Regardless the effectiveness of the previously mentioned strategies, one common weak point is that the system parameters are considered constant and known. This observation was behind the development and use of many adaptive robust controllers (ARCs). ARCs can be classified in two categories: direct adaptive controllers (DARC) and indirect adaptive controllers (IARC). In the first category, the direct adaptive nonlinear feedforward control is employed in [13]; although the obtained results are satisfactory, the study was conducted for a constant load and there was no interpretation of the estimated system parameters value. In [14], backstepping is used to control an electrohydraulic material testing system; repetitive learning is introduced in order to compensate for the system aging; this consists in linearizing the system model and using a repetitive control signal. On the other side, [15] uses a direct adaptive nonlinear control for an electrohydraulic system driven by a single-rod actuator; in this paper, the system uncertainty was estimated, along with the parameters estimation. The same approach is used in [16] for a single-rod actuator; besides the high amplitude control signal, one can see that the estimated parameter values do not reflect the physical values since they vary with the desired trajectory. Another direct adaptive control strategy based on sliding mode is used on an electrohydraulic active suspension in [17]; one can notice the long transient state for parameters convergence as well as some estimated parameters that converge to physically impossible values.

In the category of IARC, indirect adaptive control for speed and position feedback of hydraulic actuators is implemented in [18] and [19]. An integrated direct/indirect ARC is adopted in [20] and [21]; although the parameters identification convergence is reasonable, a long transient state precedes the convergence. On the other side, an indirect adaptive backstepping controller is used in [22] for a hydraulic robot arm; despite the successful control and parameters identification, the experiment was conducted for a very low amplitude and slow desired trajectory.

Both DARC and IARC have their advantages and drawback, but one thing is sure that DARC cannot separate the control law design from the parameters estimation law where the identification algorithm is limited to the gradient type. Hence, the estimated parameters in DARC are not accurate enough to be used for predictions and machine aging monitoring.

This paper proposes an indirect adaptive backstepping approach for the position control of an electrohydraulic servo system, which, on one hand, allows us to take advantage of the robust backstepping strategy, and, on the other, considers the system parameters variation, constituting thus a continuation to our study in [11] and [23]. The main concern in this paper is the identification and variation of the system parameters with the operating conditions. The benefit of using indirect adaptive control is that it guarantees the convergence of the system parameters to their real physical values, while simultaneously ensuring the system stability.

The remainder of this paper is organized as follows. The motivation for this paper is presented in Section II$. Section III presents a brief description of the mathematical model used. Section IV deals with the identification algorithm and the adaptive controller design. In Section V, experimental results are compared with a nonadaptive backstepping controller and other existing works. Finally, some conclusions and remarks conclude this paper in Section VI.

Manuscript received September 29, 2009; revised February 18, 2010 and July 14, 2010; accepted November 6, 2010. Date of publication December 30, 2010; date of current version September 7, 2011. Recommended by Technical Editor T.-C. Tsao.

The authors are with the École de Technologie Supérieure, Montreal, QC H3C 1K3, Canada (e-mail: claude.kaddissi@etsmtl.ca; maarouf.saad@etsmtl.ca; jean-pierre.kenne@etsmtl.ca).

Color versions of one or more of the figures in this paper are available online at http://ieeexplore.ieee.org.

Digital Object Identifier 10.1109/TMECH.2010.2092785

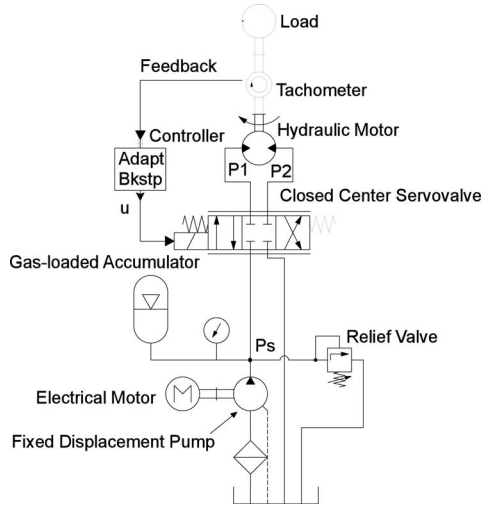

Fig. 1. Schematic of the hydraulic servosystem.

II. Motivation

Electrohydraulic systems have many applications that are of great interest. In fact, it is a real challenge to find an ideal control strategy that combines all solutions, which is why in our previous work [11], the focus was on the nonlinear and nondifferentiable aspects of the mathematical model and how they were managed by the backstepping controller. Another issue was the fine tuning of the controller parameters in order to ensure a good tracking of the reference signal. This paper for its part focuses on the hydraulic system parameters and the effect of their variation on the closed loop system behavior. For example, temperature variation affects the viscosity and bulk modulus; therefore, it can have a considerable effect, among other factors, on the system parameters. That is why we found it intriguing to develop an indirect adaptive version of the backstepping controller. Fig. 3 illustrates a block diagram of the closed loop system, which will be discussed in greater detail throughout the remainder of the paper.

III. Electrohydraulic System Modeling

The electrohydraulic test bench that was used to conduct this paper is represented in Fig. 1. Fig. 2, on the other hand, shows the photograph of the experimental equipment used.

The dc electric motor {1} drives pump {2} at a constant speed. Pump {2} has a fixed displacement, and delivers oil flow from tank {5} to the rest of the system. Normally, the pressure P_s at the pump discharge is kept constant by the mean of accumulator {3} and relief valve {4}. The installed accumulator is used as an additional source of hydraulic fluid and as a water hammer absorber. The relief valve is set to P_s, and compensates for the pressure increase due to large loads by returning the required additional amount of flow to tank {5}. The hydraulic motor {6} that drives the load has a fixed displacement; its direction of motion, speed, and acceleration are determined by the two-stage symmetric servovalve with matched orifices {7}. The load is generated through pump {8a}, which is driven by the hydraulic motor and controlled by servovalve {8b} that can create a restriction at pump {8a} discharge. All data are collected through the installed sensors: torque meter {9}, tachometer, {10} and pressure sensors {11}.

Following is a list of the electrohydraulic system parameters:

- u servovalve control input, V;
- K servovalve constant gain, cm^2/V;
- τ_v servovalve time constant, s;

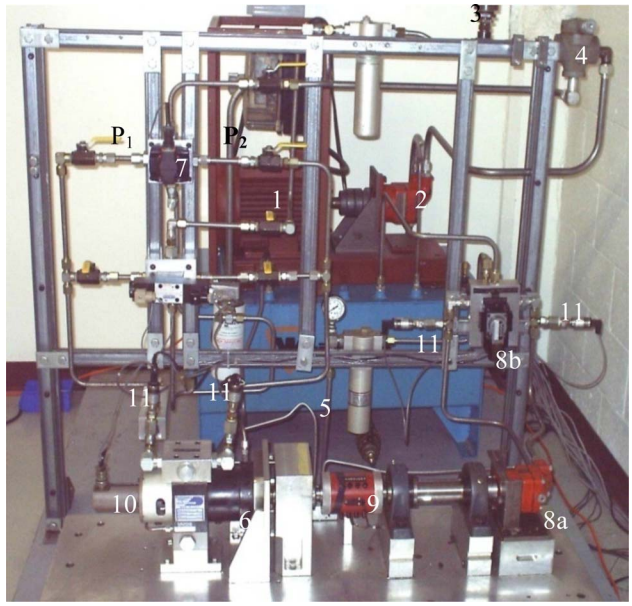

Fig. 2. Experimental electrohydraulic workbench.

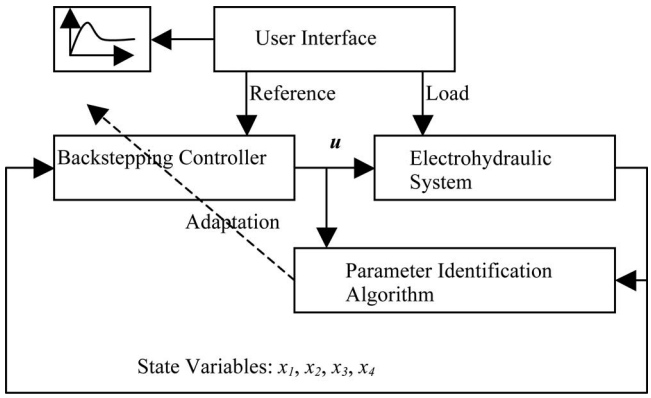

Fig. 3. Indirect adaptive backstepping controller.

- A_v servovalve orifice opening area, cm^2;
- Q flow rates to and from the servovalve, cm^3/s;
- $P_{1,2}$ pressures in the actuator chambers, bars;
- P_L pressure differential due to load, bars;
- P_s pressure at the pump discharge, bars;
- C_d flow discharge coefficient, dimensionless;
- ρ fluid oil mass density, g/cm^3;
- C_L load leakage coefficient, cm^5/daN·s;
- β fluid bulk modulus, bars;
- V oil volume in one chamber of the actuator, cm^3;
- D_m actuator volumetric displacement, cm^3/rad;
- T_L load torque, daN ·cm;
- B viscous damping coefficient, daN·cm·s;
- J actuator inertia, daN·s^2·cm;
- θ_p actuator angular position, rad.

The system units are chosen such as to avoid numerical errors. The flow through the servovalve is given by

$$Q = C_d A_v \sqrt{\frac{P_s - P_L}{\rho}}, \qquad \text{if } \dot{\theta}_p > 0 \tag{1}$$

$$Q = C_d A_v \sqrt{\frac{P_s + P_L}{\rho}}, \qquad \text{if } \dot{\theta}_p < 0. \tag{2}$$

Therefore, since $\operatorname{sign}(A_v) = \operatorname{sign}\left(\dot{\theta}_p\right)$, we can write

$$Q = C_d A_v \sqrt{\frac{P_s - \operatorname{sign}(A_v) P_L}{\rho}} \tag{3}$$

where $P_s = P_1 + P_2$ and $P_L = P_1 - P_2$, since the servovalve is symmetric with matched orifices [1].

In order to avoid numerical problems due the nondifferentiable term in (3), we approximated the sign function with a sigmoid function having the following properties:

$$\operatorname{sigm}(x) = \frac{1 - e^{ax}}{1 + e^{ax}} \qquad \forall x \in \Re. \tag{4}$$

This is a continuously differentiable function with

$$a > 0 \quad \text{and} \quad \operatorname{sigm}(x) = \begin{cases} 1, & \text{if } ax \to \infty \\ 0, & \text{if } ax \to 0 \\ -1, & \text{if } ax \to -\infty \end{cases}. \tag{5}$$

The effect of the invariant set induced by (4) can be remedied by choosing an appropriate value for the positive constant a.

Hence,

$$Q = C_d A_v \sqrt{\frac{P_s - \operatorname{sigm}(A_v) P_L}{\rho}}. \tag{6}$$

This approximation guarantees the existence of a solution independent of the actuator rotation direction. On the other hand, since hydraulic oil is compressible to some limits; it should be considered in the actuator dynamics. Thus, we give the compressibility equation as follows:

$$\frac{V}{2\beta} \dot{P}_L = \frac{C_d A_v}{\sqrt{\rho}} g(.) - D_m \dot{\theta} - C_L P_L \tag{7a}$$

where

$$g(.) = \sqrt{P_s - \operatorname{sigm}(A_v) P_L}. \tag{7b}$$

Let us now consider the hydraulic actuator equation of motion given by Newton's second law; we have

$$J \ddot{\theta}_p = D_m (P_1 - P_2) - B \dot{\theta}_p - T_L. \tag{8}$$

In (8), the Coulomb friction was neglected since the hydraulic motor that is used is small relatively to the hydraulic power carried by the fluid flow, even at small speeds.

The final remaining component is the servovalve. Its dynamic equation is a first-order one, since its spool inertia has been neglected for simplification purposes. It is given by

$$\tau_v \dot{A}_v + A_v = K u. \tag{9}$$

More details can be found about the electrohydraulic system modeling in our previous work [11].

Now, if we choose $x_1 = \theta_p$, $x_2 = \omega = \dot{\theta}_p$, $x_3 = P_L$, and $x_4 = A_v$ as state variables, the system can be written in a fourth-order nonlinear state-space model

$$\begin{cases} \dot{x}_1 = x_2 \\ \dot{x}_2 = w_a x_3 - w_b x_2 - w_c \\ \dot{x}_3 = p_a x_4 \sqrt{P_s - x_3 \operatorname{sigm}(x_4)} - p_b x_3 - p_c x_2 \\ \dot{x}_4 = -r_a x_4 + r_b u \end{cases} \tag{10}$$

where r_a, r_b, p_a, p_b, p_c, w_a, w_b, and w_c are the system parameters given by

$$r_a = \frac{1}{\tau_v} \quad r_b = \frac{K}{\tau_v} \quad p_a = \frac{2\beta C_d}{V\sqrt{\rho}} \quad p_a = \frac{2\beta C_L}{V}$$
$$p_c = \frac{2\beta D_m}{V} \quad w_a = \frac{D_m}{J} \quad w_b = \frac{B}{J} \quad w_c = \frac{T_L}{J}.$$

The parameters r_a and r_b are known and provided by the servovalve datasheet (refer to Section V). The parameters covered by the identification process are p_a, p_b, p_c, w_a, w_b, *and* w_c. Those parameters are unknown but fairly time invariant and will be continuously identified during the control process, and then injected into the backstepping controller, as shown in Fig. 3. The next step is to set up and design the indirect adaptive backstepping controller.

IV. Indirect Adaptive Backstepping Controller

Referring to Fig. 3, the control of the electrohydraulic system is achieved as follows:

1) The state variables x_1, x_2, x_3, and x_4 are sent to the parameter identification block along with the control signal u.
2) Once the system parameters are identified, they are introduced into the backstepping controller block as well as the four-state variables to generate the control signal.
3) The control signal is brought to the electrohydraulic system forcing the hydraulic actuator to track the desired trajectory x_{ref}, taking into consideration the resistive load.

This sequence is repeated for each sampling time. Note that the reference signal x_{ref} must be at least a Class-C4 function since its fourth-order derivative appears in the control signal equation, as we will see later on.

Based on (10), we can write (11) and (12)

$$\begin{cases} \dot{x}_2 = w_a x_3 - w_b x_2 - w_c \\ \dot{x}_3 = p_a x_4 g(.) - p_b x_3 - p_c x_2 \end{cases} \tag{11}$$

$$\begin{pmatrix} \dot{x}_2 \\ \dot{x}_3 \end{pmatrix} = \begin{pmatrix} x_3 & 0 \\ -x_2 & 0 \\ -1 & 0 \\ 0 & x_4 g(.) \\ 0 & -x_3 \\ 0 & -x_2 \end{pmatrix}^T \times \begin{pmatrix} w_a \\ w_b \\ w_c \\ p_a \\ p_b \\ p_c \end{pmatrix}. \tag{12}$$

It can be seen that the subsystem (12) is linear with respect to its parameters, which is a sufficient condition for the parameters to be identified through the continuous recursive least-squares method for slowly varying systems [24]. The latter is among the unbiased identification methods, and with the addition of a low power white noise signal to the closed loop system input, the parameters will converge asymptotically to their real value. So, let

$$y(t) = \begin{pmatrix} \dot{x}_2 \\ \dot{x}_3 \end{pmatrix} \tag{13a}$$

$$\varphi(t) = \begin{pmatrix} x_3 & -x_2 & -1 & 0 & 0 & 0 \\ 0 & 0 & 0 & x_4 g(.) & -x_3 & -x_2 \end{pmatrix} \tag{13b}$$

$$\theta^T = \begin{pmatrix} w_a & w_b & w_c & p_a & p_b & p_c \end{pmatrix} \tag{13c}$$

where *y(t)* is the observation vector, *φ(t)* is the matrix of regressors, and θ is the vector of unknown parameters that are continuously identified. Then,

$$y(t) = \varphi(t)\theta. \tag{14}$$

Next, we define the least-squares error $V(\theta)$ and the matrix *P(t)* as well, according to [23],

$$\begin{cases} V(\theta) = \int_0^t e^{\alpha(t-T)} \left(y(T) - \varphi(T)\theta(T)\right)^2 dT \\ \alpha(t_n) = 1 - \lambda(1 - \alpha(t_{n-1})) : \text{Weighting factor,} \\ \quad \text{with } \lambda = 0.99 \\ P(t) = \left(\int_0^t \varphi(T)\varphi(T)^T dT\right)^{-1}. \end{cases} \tag{15a}$$

We also define the estimated system parameters as follows:

$$\hat{\theta}^T = (\,\hat{w}_a \quad \hat{w}_b \quad \hat{w}_c \quad \hat{p}_a \quad \hat{p}_b \quad \hat{p}_c\,). \tag{15b}$$

Let $\tilde{\theta}$ be the parameter estimation error and $\breve{\theta} = \hat{\theta} + \tilde{\theta}$ the true value of θ; thus,

$$\breve{\theta} = \Bigg(\underbrace{\hat{w}_a + \tilde{w}_a}_{\breve{w}_a} \quad \underbrace{\hat{w}_b + \tilde{w}_b}_{\breve{w}_b} \quad \underbrace{\hat{w}_c + \tilde{w}_c}_{\breve{w}_c} \quad \underbrace{\hat{p}_a + \tilde{p}_a}_{\breve{p}_a} \quad \underbrace{\hat{p}_b + \tilde{p}_b}_{\breve{p}_b} \quad \underbrace{\hat{p}_c + \tilde{p}_c}_{\breve{p}_c} \Bigg). \tag{15c}$$

Identification is carried on until the value of $\tilde{\theta}$ minimizes the least-squares error, according to [23], and satisfies the following conditions:

$$\begin{cases} \dfrac{d\hat{\theta}(t)}{dt} = P(t)\varphi(t)^T e(t) \\ e(t) = y(t) - \varphi(t)\hat{\theta} = \varphi(t)\left(\theta - \hat{\theta}\right) = \varphi(t)\tilde{\theta}\ . \\ \dfrac{dP(t)}{dt} = \alpha P(t) - P(t)\varphi(t)^T\varphi(t)P(t) \end{cases} \tag{16}$$

By integrating the first equation of (16), we get the estimates of the system parameters.

Finally, to close the loop in Fig. 3, the backstepping controller block is designed based on [25]; its tuning parameters are listed in the Appendix .

Let $e_i = x_i - x_{id}$ be the tracking error between every state variable and its desired value.

Let $f_i(\tilde{\theta}, \dot{\tilde{\theta}})$ be the functions that group the parameter estimation errors and their derivatives.

Step 1: Let $V_1 = \frac{1}{2\rho_1}e_1^2$ be a candidate Lyapunov function for the subsystem $\dot{x}_1 = x_2$ of (10). Then,

$$\dot{V}_1 = \frac{e_1}{\rho_1}(\dot{x}_1 - \dot{x}_{1d}) = \frac{e_1}{\rho_1}(x_2 - \dot{x}_{1d}). \tag{17}$$

If we choose the following stabilizing function, as the desired value for x_2 in (17):

$$x_{2d}(e_1, x_{1d}) = \dot{x}_{1d} - \rho_1 e_1 \tag{18}$$

this will yield

$$\dot{V}_1 = -e_1^2 + \frac{e_1 e_2}{\rho_1}. \tag{19}$$

Step 2: Let $V_2 = (1/2\rho_1)e_1^2 + (1/2\rho_2)e_2^2$ be a candidate Lyapunov function for the subsystem; $\dot{x}_2 = \breve{w}_a x_3 - \breve{w}_b x_2 - \breve{w}_c$ then,

$$\dot{V}_2 = -e_1^2 + e_2\left\{\frac{\hat{w}_a}{\rho_2}x_3 + \left(\frac{1}{\rho_1} + \frac{(\hat{w}_b - \rho_1)\rho_1}{\rho_2}\right)e_1 + \frac{(\rho_1 - \hat{w}_b)}{\rho_2}e_2 - \frac{\hat{w}_b}{\rho_2}\dot{x}_{1d} - \frac{\ddot{x}_{1d}}{\rho_2} - \frac{\hat{w}_c}{\rho_2} + f_2(\tilde{\theta})\right\}. \tag{20}$$

If we choose the following stabilizing function, as the desired value for x_3 in (20):

$$x_{3d}(e_1, e_2, \dot{x}_{1d}, \ddot{x}_{1d}) = \left\{-a_1 e_1 - a_2 e_2 + \frac{\hat{w}_b}{\hat{w}_a}\dot{x}_{1d} + \frac{\ddot{x}_{1d}}{\hat{w}_a} + \frac{\hat{w}_c}{\hat{w}_a}\right\} \tag{21a}$$

where

$$a_1 = \frac{\rho_2}{\rho_1\hat{w}_a} + \frac{(\hat{w}_b - \rho_1)\rho_1}{\hat{w}_a}$$

and

$$a_2 = \frac{\rho_1 - \hat{w}_b + \rho_2}{\hat{w}_a}. \tag{21b}$$

Thus,

$$\dot{V}_2 = -e_1^2 - e_2^2 + \frac{\hat{w}_a}{\rho_2}e_2 e_3 + e_2 f_2(\tilde{\theta}). \tag{22}$$

Step 3: Let $e_3 = x_3 - x_{3d}$ and $V_3 = (1/2\rho_1)e_1^2 + (1/2\rho_2)e_2^2 + (1/2\rho_3)e_3^2$ be a candidate Lyapunov function for the subsystem $\dot{x}_3 = \breve{p}_a x_4 g(.) - \breve{p}_b x_3 - \breve{p}_c x_2$; then

$$\dot{V}_3 = -e_1^2 - e_2^2 + e_3 \times \left\{\begin{array}{c} \dfrac{\hat{p}_a C_d x_4 g(.)}{\rho_3} + \dfrac{b_1 - b_6}{\rho_3}e_1 + \left(\dfrac{b_2 - b_7}{\rho_3} + \dfrac{\hat{w}_a}{\rho_2}\right)e_2 \\ + \dfrac{b_3}{\rho_3}e_3 + \dfrac{b_8 - b_4}{\rho_3}\dot{x}_{1d} - \dfrac{b_5}{\rho_3} + \dfrac{\dot{\hat{w}}_a}{\rho_3\hat{w}_a^2}\ddot{x}_{1d} \\ - \dfrac{\dddot{x}_{1d}}{\rho_3\hat{w}_a} - b_{10} + f_3(\tilde{\theta}, \dot{\tilde{\theta}}) \end{array}\right\} \tag{23a}$$

where

$$\begin{cases} b_1 = \hat{p}_b a_1 + \hat{p}_c\rho_1 - a_1\rho_1 - \rho_2/\rho_1 \\ b_2 = \hat{p}_b a_2 - \hat{p}_c + a_1 - \rho_2 a_2 \\ b_3 = \hat{p}_a a_2 - \hat{p}_b \\ b_4 = \hat{p}_b\hat{p}_b/\hat{p}_a + \hat{p}_c \\ b_5 = (\hat{p}_b + \hat{p}_b)/\hat{p}_a \\ b_6 = \rho_2\dot{\hat{w}}_a/\rho_1\hat{w}_a^2 + \left[\rho_1\dot{\hat{w}}_b\hat{w}_a - \rho_1\dot{\hat{w}}_a(\hat{w}_b - \rho_2)\right]/\hat{w}_a^2 \\ b_7 = \left[-\dot{\hat{w}}_b\hat{w}_a - \dot{\hat{w}}_a(\rho_1 + \rho_2 - \hat{w}_b)\right]/\hat{w}_a^2 \\ b_8 = \left(\dot{\hat{w}}_b\hat{w}_a - \dot{\hat{w}}_a\hat{w}_b\right)/\hat{w}_a^2 \\ b_9 = \left(\dot{\hat{w}}_c\hat{w}_a - \dot{\hat{w}}_a\hat{w}_c\right)/\hat{w}_a^2 \\ b_{10} = \hat{p}_b\hat{w}_c/\rho_3\hat{w}_a + b_9/\rho_3 \end{cases} \tag{23b}$$

If we choose the following stabilizing function, as the desired value for x_3 in (23a)

$$x_{4d}(e_1, e_2, e_3, \dot{x}_{1d}, \ddot{x}_{1d}, \dddot{x}_{1d}) = \frac{1}{\hat{p}_a C_d g(.)}\left\{-(b_1 - b_6)e_1 - \left(b_2 - b_7 + \frac{\rho_3\hat{w}_a}{\rho_2}\right)e_2 - b_3 e_3 - (b_8 - b_4)\dot{x}_{1d} + \left(b_5 + \frac{\dot{\hat{w}}_a}{\hat{w}_a^2}\right)\ddot{x}_{1d} + \frac{\dddot{x}_{1d}}{\hat{w}_a} + b_{10} - \rho_3 e_3\right\}. \tag{24}$$

Thus,

$$\dot{V}_3 = -e_1^2 - e_2^2 - e_3^2 + \frac{\hat{p}_a C_d g(.)}{\rho_3}e_3 e_4 + e_3 f_3(\tilde{\theta}, \dot{\tilde{\theta}}). \tag{25}$$

At this stage, the stabilizing functions, which are the desired trajectories of all the state variables, have been designed. Every stabilizing function depends on the tracking error of the previous states, on the desired position, and on its derivatives.

Final step: The final step involves the design of the control signal, which is the electric signal that actuates the servovalve. Let $V_4 = (1/2\rho_1)e_1^2 + (1/2\rho_2)e_2^2 + (1/2\rho_3)e_3^2 + (1/2\rho_4)e_4^2$ be a candi-

date Lyapunov function for the subsystem $\dot{x}_4 = -r_a x_4 + r_b u$; then

$$\dot{V}_4 = -e_1^2 - e_2^2 - e_3^2 + e_4 \left\{ \frac{r_b}{\rho_4} \left(1 - \frac{x_3 f(.) h(.)}{2\hat{p}_a C_d \rho . g(.)^3} \right) u + \frac{\hat{p}_a C_d g(.) e_3}{\rho_3} - \frac{r_a}{\rho_4} x_4 - \frac{J(.)}{\rho_4 \hat{p}_a C_d g(.)} - \frac{1}{2\hat{p}_a C_d \rho_4 \rho . g(.)^3} \{ \dot{x}_3 \mathrm{sgm}(x_4) - r_a x_3 x_4 f(.) \} h(.) \right\} + f_4(\tilde{\theta}, \dot{\tilde{\theta}}, \ddot{\tilde{\theta}}) \tag{26a}$$

where

$$\begin{cases} f(.) = \partial(\mathrm{sgm} x_4)/\partial x_4 = 2a e^{-a x_4}/(1 + e^{-a x_4})^2 \\ h(.) = -b_1 e_1 - c_1 e_2 - c_2 e_3 + b_4 \dot{x}_{1d} + b_5 \ddot{x}_{1d} + \dddot{x}_{1d}/\hat{w}_a + p_b \hat{w}_c/\hat{w}_a \\ J(.) = (d_1 - \dot{b}_1 + \dot{b}_6) e_1 + (d_2 - \dot{b}_2 + \dot{b}_7 - \dot{\hat{w}}_a/\rho_2) e_2 \\ \quad + (d_3 - \dot{b}_3) e_3 - c_2 \hat{p}_a C_d g(.) e_4 + x_{1d}^{(4)}/\hat{w}_a \\ \quad + (b_5 + \dot{\hat{w}}_a/\hat{w}_a^2) \dddot{x}_{1d} \\ \quad + [b_4 + \dot{b}_5 + (\ddot{\hat{w}}_a \hat{w}_a^2 - 2\hat{w}_a \dot{\hat{w}}_a^2)/\hat{w}_a^4] \ddot{x}_{1d} \\ \quad - (\dot{b}_8 - \dot{b}_4) \dot{x}_{1d} + \dot{b}_{10} \end{cases}$$

and

$$\begin{cases} c_1 = b_2 + \rho_3 \hat{w}_a/\rho_2 \\ c_2 = b_3 + \rho_3 \\ d_1 = b_1 \rho_1 + \rho_2 c_1/\rho_1 \\ d_2 = -b_1 + c_1 \rho_2 + \rho_3 c_2 \hat{w}_a/\rho_2 \\ d_3 = -c_1 \hat{w}_a + c_2 \rho_3 . \end{cases} \tag{26b}$$

Now, we choose the control signal u in (26a) as shown by (27) at the bottom of this page. Thus,

$$\dot{V}_4 = -e_1^2 - e_2^2 - e_3^2 - e_4^2 + f_4(\tilde{\theta}, \dot{\tilde{\theta}}, \ddot{\tilde{\theta}}). \tag{28}$$

It can be shown that $f_4(\tilde{\theta}, \dot{\tilde{\theta}}, \ddot{\tilde{\theta}})$ tends to zero when θ converges toward $\hat{\theta}$ [25]. At that moment, (28) becomes strictly negative.

This shows that the error dynamic is globally asymptotically stable, because any error signal will converge to zero.

Finally, if the system model (10) can be written in terms of the closed loop tracking errors $e_i = x_i - x_{\mathrm{id}}$ to reflect the error dynamics as follows:

$$(\dot{e}_1 \quad \dot{e}_2 \quad \dot{e}_3 \quad \dot{e}_4)^T = A (e_1 \quad e_2 \quad e_3 \quad e_4)^T \tag{29a}$$

where

$$A = \begin{pmatrix} -\rho_1 & 1 & 0 & 0 \\ -\frac{\rho_2}{\rho_1} & -\rho_2 & \hat{w}_a & 0 \\ 0 & -\frac{\rho_3}{\rho_2} \hat{w}_a & -\rho_3 & \hat{p}_a C_d g(.) \\ 0 & 0 & -\frac{\rho_4}{\rho_3} \hat{p}_a C_d g(.) & -\rho_4 \end{pmatrix}. \tag{29b}$$

V. Experimental Results

Regarding the details of the real-time computing system, refer to [11]. The servovalve time constant is 0.02 s; this is the smallest time constant among all components. Therefore, in order to have good data acquisition, the sampling rate for such a system must be roughly ten times smaller which means 1 ms. However, because of the heavy amount of calculations and the discretization method that was used (fourth-order Runge–Kutta method), sampling times larger than 0.1 ms did not yield to the expected performance. Therefore, a sampling time of 0.1 ms was used and the control signal was updated at the same rate. The actuator angular speed is measured by a 48.1-r/min/V tachometer; the angular position was obtained by integrating the angular speed. The supply pressure P_s is set at 7 MPa; pressures P_1 and P_2 at the hydraulic actuator inlet and outlet, respectively, are measured with two electrical manometers of 2 MPa/V_{dc}. The servovalve opening was measured by its spool position sensor with a constant gain of 0.0265 cm^2/V. The desired angular position trajectory is a sine function with a 2π rad amplitude and a 2-Hz frequency. A white noise signal with as low power of 0.02 dB·W was added to the desired position in order to provide the signal with a wide range of frequencies without, however, perturbing the system output. This is crucial for good unbiased parameters identification. Also, for a faster identification, the matrix P initial value should be high enough and was set to $5000 * I_6$. Fig. 4 shows the angular position, the desired position, and the tracking error. At instant 12.24 s, the load on the actuator was increased abruptly to ten times its nominal value (57 N·m), as we can see the adaptive controller achieves very good tracking with a maximum error around 1/40 πrad. However, because of the adaptive control, the desired position is once more attained quite in only 0.07 s. At the same time, in Fig. 5, we

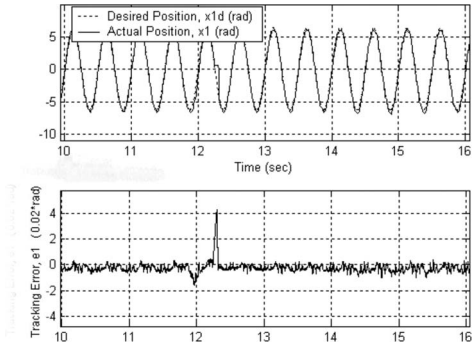

Fig. 4. Angular position, desired position, and tracking error, when using the indirect adaptive backstepping during sudden load increase.

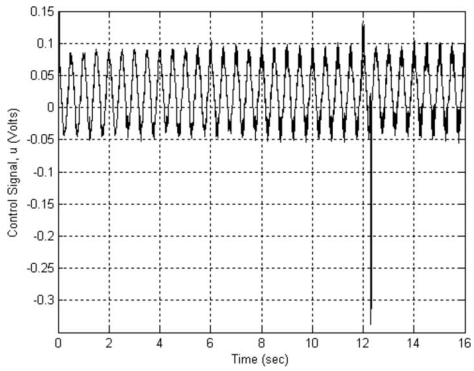

Fig. 5. Control signal of the indirect adaptive backstepping controller.

$$u(e_1, e_2, e_3, e_4, \dot{x}_{1d}, \ddot{x}_{1d}, \dddot{x}_{1d}, x_{1d}^{(4)}) = \frac{\left\{ -\rho_4/\rho_3 . \hat{p}_a C_d g(.) e_3 + r_a x_4 + J(.)/\hat{p}_a C_d g(.) + 1/2\hat{p}_a C_d \rho . g(.)^3 \left\{ \dot{x}_3 \mathrm{sgm}(x_4) - r_a x_3 x_4 f(.) \right\} h(.) - \rho_4 e_4 \right\}}{r_b \left(1 - x_3 f(.) h(.)/2\hat{p}_a C_d \rho . g(.)^3 \right)}. \tag{27}$$

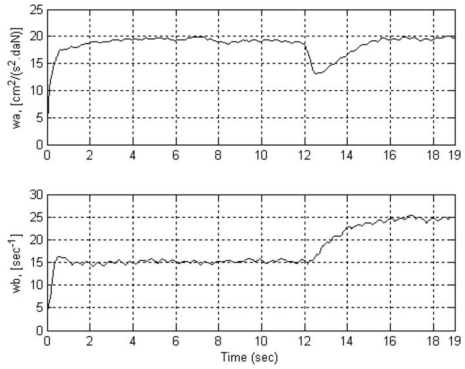

Fig. 6. Parameters of the hydraulic motor: motor displacement and friction.

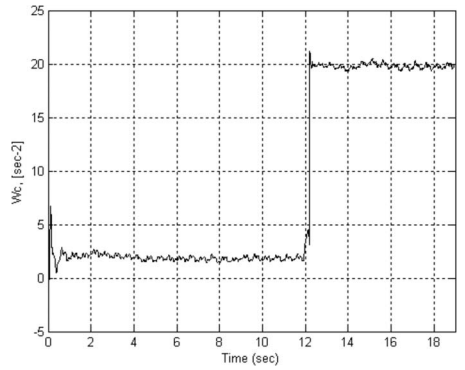

Fig. 7. Parameter w_c (proportional to the resistive torque T_L).

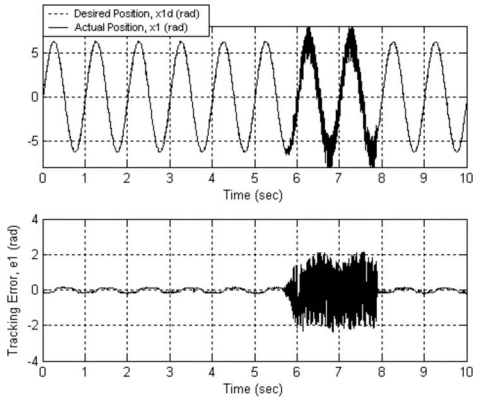

Fig. 8. Angular position, desired position, and tracking error when using a nonadaptive backstepping.

can see the peak of voltage (-0.34 V) in the control signal, due to the load increase, and the ability of the adaptive controller to restore the former signal amplitude. Let us now examine the identification of the parameters and their behavior during the sudden load increase. Fig. 6 illustrates the convergence of the hydraulic motor parameters w_a and w_b that are proportional to the motor displacement and friction coefficient, respectively. It is clear that the identification has achieved a good convergence of the parameters toward their physical values. In fact, w_a regains its value shortly after the sudden load increase; however, w_b converges toward a higher value since the friction coefficient increases with load.

On the other hand, the hydraulic parameters p_a, p_b, and p_c that are proportional to the oil bulk modulus have a very similar behavior as well; this is why they are not shown. Fig. 7 shows parameter w_c that

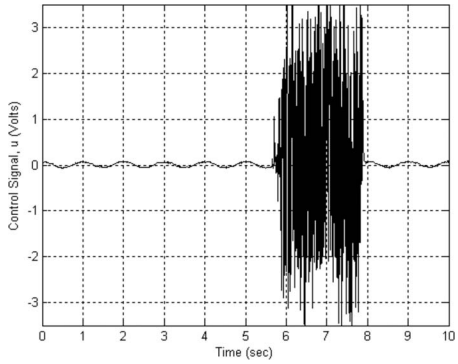

Fig. 9. Control signal of the nonadaptive backstepping controller.

is proportional to resistive torque T_L, as we can see, after the abrupt load increase, w_c converges to a new value which is fairly ten times its previous value (from 2 to 20 s^{-2}). For all identified parameters, we can see from Figs. 6 and 7 that convergence is reached in roughly 1 s in the phase preceding the load increase, as compared to 4 s in [17] and 10 s in [20]. Finally, Figs. 8 and 9 study the behavior of the nonadaptive backstepping controller, using the same control parameters value, as the adaptive controller (Appendix). Although the desired position in this case is smoother and has a frequency of 1 Hz, when the load on the hydraulic actuator is set to ten times its nominal value, the tracking is lost and the actuator oscillates continuously (see Fig. 8) along with a saturated control signal (see Fig. 9).

VI. Conclusion

In this paper, an indirect adaptive backstepping controller was designed for an experimental electrohydraulic test bench. It is well known that electrohydraulic systems parameters are subjected to variations, depending on the system load, pressure, and temperature. The results were compared to those obtained with a real-time nonadaptive backstepping controller as well as to results from other similar works. We saw that during parameter variations, the adaptive controller was able to track the desired reference signal with a slight transient behavior after the parameters variation. On the other hand, the nonadaptive controller was unable to keep the system on track, and ended up with large oscillations and instability. This paper is an added value to the existing literature since few references are available for IARC as applied to electrohydraulic systems, because its implementation constitutes a big challenge. We were able to show and prove that IARC is the ideal option for hydraulic systems control, since it leads to the real physical values of the system parameters, which allows a good system monitoring.

Appendix

List of the Controller Tuning Parameters

Controller parameters	Value	Observations
ρ_1	50	---
ρ_2	150	$\rho_2 > \rho_1$ since speed must converge faster than position
ρ_3	40	$\rho_3 < \rho_2$ to minimize the effect of w_a in (29')
ρ_4	0.001	$\rho_4 << \rho_3$ to minimize the effect of $p_a C_d g(.)$ in (29')

REFERENCES

[1] H. E. Merrit, *Hydraulic Control Systems:*. New York: Wiely, 1967.

[2] S. Habibi and A. Goldenberg, "Design of a new high-performance electrohydraulic actuator," *IEEE/ASME Trans. Mechatronics*, vol. 5, no. 2, pp. 158–164, Jun. 2000.

[3] P. Y. Li, "Dynamic redesign of a flow control servo-valve using a pressure control pilot," presented at the ASME Int. Mech. Eng. Congr. Expos., New York, NY, Nov 11–16, 2001.

[4] M. K. Zavarehi, P. D. Lawrence, and F. Sassani, "Nonlinear modeling and validation of solenoid-controlled pilot-operated servovalves," *IEEE/ASME Trans. Mechatronics.*, vol. 4, no. 3, pp. 324–334, Sep. 1999.

[5] S. LeQuoc, R. M. H. Cheng, and K. H. Leung, "Tuning an electrohydraulic servovalve to obtain a high amplitude ratio and a low resonance peak," *J. Fluid Control*, vol. 20, pp. 30–49, 1990.

[6] T. J. Lim, "Pole placement control of an electro-hydraulic servo motor," presented at the 2nd Int. Conf. Power Electronics and Drive Systems, PEDS. Part 1 (of 2), Singapore, Singapore, May 26–29, 1997.

[7] W. Zeng and J. Hu, "Application of intelligent PDF control algorithm to an electrohydraulic position servo system," in *Proc. IEEE/ASME Inter. Conf. Adv. Intel. Mechatronics (AIM'99), Atlanta, GA*, Sep.19–23,, pp. 233–238.

[8] A. Fink and T. Singh, "Discrete sliding mode controller for pressure control with an electrohydraulic servovalve," presented at the IEEE Int. Conf. Control Appl. Part 1 (of 2), Trieste, Italy, Sep. 1–4, 1998.

[9] H.-M. Chen, J.-C. Renn, and J.-P. Su, "Sliding mode control with varying boundary layers for an electro-hydraulic position servo system," *Int. J. Adv. Manuf. Technol.*, vol. 26, pp. 117–123, 2005.

[10] H. Hahn, A. Piepenbrink, and K.-D. Leimbach, "Input/output linearization control of an electro servo-hydraulic actuator," presented at the IEEE Conf. Control. Appl. Part 2 (of 3), Glasgow, U.K., Aug. 24–26, 1994.

[11] C. Kaddissi, J.-P. Kenné, and M. Saad, "Identification and real-time control of an electrohydraulic servo system based on nonlinear backstepping," *IEEE/ASME Trans. Mechatronics*, vol. 12, no. 1, pp. 12–22, Feb. 2007.

[12] R. Liu and A. Alleyne, "Nonlinear force/pressure tracking of an electrohydraulic actuator," *J. Dynam. Syst., Meas. Control*, vol. 122, no. 1, pp. 232–237, 2000.

[13] C. Tai, T.-C. Tsao, and M. B. Levin, "Adaptive nonlinear feedforward control of an electrohydraulic camless valvetrain," presented at the Amer. Control Conf., Chicago, IL, Jun. 2000.

[14] S. J. Lee and T.-C. Tsao, "Repetitive learning of backstepping controlled nonlinear electrohydraulic material testing system," *IFAC J. Control Eng. Pract.*, vol. 12, no. 11, pp. 1393–1408, Nov. 2004.

[15] C. Guan and S. Pan, "Nonlinear Adaptive robust control of single-rod electro-hydraulic actuator with unknown nonlinear parameters," *IEEE Trans. Control Syst. Technol.*, vol. 16, no. 3, pp. 434–445, May 2008.

[16] B. Yao, F. Bu, J. Reedy, and G. T.-C. Chiu, "Adaptive robust control of single-rod hydraulic actuators: Theory and Experiments," *IEEE/ASME Trans. Mechatronics.*, vol. 5, no. 1, pp. 79–91, Mar. 2000.

[17] A. Alleyne and J. K. Hedrick, "Nonlinear adaptive control of active suspensions," *IEEE Trans. Control Syst. Technol.*., vol. 3, no. 1, pp. 94–101, Mar. 1995.

[18] W.-S. Yu and T.-S. Kuo, "Robust indirect adaptive control of the electrohydraulic velocity control systems," *IEE Proc.—Control Theory Appl.*, vol. 143, no. 5, pp. 448–454, Sep. 1996.

[19] W.-S. Yu and T.-S. Kuo, "Continuous-time indirect adaptive control of the electrohydraulic servo systems," *IEEE Trans. Control Syst. Technol.*, vol. 5, no. 2, pp. 163–177, Mar. 1997.

[20] A. Mohanty, B. Yao. (2010, Jul.). "Integrated direct/indirect adaptive robust control of hydraulic manipulators with valve deadband," *IEEE/ASME Trans. Mechatronics,* [Online]. Available: http://ieeexplore.ieee.org, DOI: 10.1109/TMECH.2010.2051037.

[21] M.K. Ciliz, "Combined direct and indirect adaptive control for a class of nonlinear systems," *Control Theory Appl.*, vol. 3, no. 1, pp. 151–159, Jan. 2009.

[22] A. Mohanty, B. Yao. (2010, May). "Indirect adaptive robust control of hydraulic manipulators with accurate parameter estimates," *IEEE Trans. Control Syst. Technol.,* [Online]. Available: http://ieeexplore.ieee.org, DOI: 10.1109/TCST.2010.2048569.

[23] C. Kaddissi, J.-P. Kenne, and M. Saad, "Indirect adaptive control of an electrohydraulic servo system based on nonlinear backstepping," presented At the IEEE Int. Symp. Industrial Electronics., Montreal, QC, Canada, 2006.

[24] K. J. Astrom and B. Wittenmark, *Adaptive Control*. Reading, MA: Addison-Wesley, 1989.

[25] M. Krstic, I. Kanellakopoulos, and P. V. Kokotovic, *Nonlinear and Adaptive Control Design*. New York: Wiley, 1995.